Frontiers in Bioscience Landmark

Front. Biosci. (Landmark Ed) **2026**; 31(7): 51017
https://doi.org/10.31083/FBL51017

Original Research

BTG1 Mediates the Proliferation and Activation of Hepatic Stellate Cells via the JAK2/STAT3 Pathway in Liver Fibrosis

Weili Lu[1,2], Ziyi An[1], Muran Lu[1], Jinling Kong[1], Li Wang[1], Xiaowen Feng[1,*], Fanrong Wu[1,2,*]

[1]Inflammation and Immune Mediated Diseases Laboratory of Anhui Province, School of Pharmacy, Anhui Medical University, 230032 Hefei, Anhui, China
[2]Department of Clinical Laboratory, The Second Hospital of Anhui Medical University, 230032 Hefei, Anhui, China
*Correspondence: fengxiaowen@ahmu.edu.cn (Xiaowen Feng); wufanrong@ahmu.edu.cn (Fanrong Wu)
Academic Editor: Christian Borgo
Submitted: 14 February 2026 Revised: 12 May 2026 Accepted: 22 May 2026 Published: 17 July 2026

Abstract

Background: Liver fibrosis is pathologically characterized by excessive extracellular matrix (ECM) deposition induced by diverse etiological factors, which is associated with hepatic stellate cell (HSC) activation and proliferation. B-cell translocation gene 1 (BTG1) contributes to the regulation of cellular proliferation, differentiation, and development. The biological role of BTG1 in HSC activation and liver fibrosis remains incompletely understood. **Methods:** To clarify the regulatory role of BTG1, carbon tetrachloride (CCl_4)-induced rat liver fibrosis models and platelet-derived growth factor-BB (PDGF-BB)-activated HSC-T6 cells were used. For *in vivo* studies, rats were injected with BTG1-overexpressing recombinant adeno-associated virus (AAV). siRNA or overexpression vectors targeting BTG1 were transfected into HSC-T6 cells *in vitro*, respectively. Rat serum alanine aminotransferase (ALT) and aspartate aminotransferase (AST) levels were measured using biochemical assays. Liver histopathological alterations were evaluated by histological staining. 5-ethynyl-2′-deoxyuridine (EdU) assays and flow cytometry were used to assess cell proliferation and apoptosis. Immunohistochemistry, Western blotting, and quantitative real-time polymerase chain reaction (RT-qPCR) were performed to quantify the levels of α-smooth muscle actin (α-SMA), collagen I, interleukin-6 (IL-6), and tumor necrosis factor-α (TNF-α), as well as proliferation- and apoptosis-related proteins. Furthermore, a specific JAK2 inhibitor was used to further clarify the underlying molecular mechanism. **Results:** BTG1 was significantly downregulated in CCl_4-induced fibrotic liver tissues and activated HSCs. AAV-mediated BTG1 overexpression markedly alleviated liver fibrosis in rats. siRNA-mediated BTG1 knockdown resulted in the significant upregulation of collagen I, α-SMA, IL-6, and TNF-α expression in HSC-T6 cells. BTG1 deficiency enhanced HSC-T6 cell proliferation induced by PDGF-BB as evidenced by increased expression of proliferating cell nuclear antigen (PCNA) and Ki67, while inhibiting apoptotic death, as evidenced by reduced levels of Bax and cleaved caspase-3, and by enhanced Bcl-2 expression. BTG1 overexpression had the opposite effects. Mechanistically, BTG1 deficiency enhanced JAK2/STAT3 signaling by upregulating the phosphorylation of these signaling intermediaries, whereas BTG1 overexpression inhibited this signaling pathway. Notably, pretreatment with the JAK2 inhibitor ruxolitinib neutralized BTG1 knockdown-induced JAK2/STAT3 hyperactivation. **Conclusions:** BTG1 suppresses HSC activation by modulating the JAK2/STAT3 signaling axis and retards liver fibrosis progression, suggesting that it may represent a promising therapeutic target for anti-fibrotic intervention.

Keywords: hepatic stellate cells; BTG1; Janus kinase 2; STAT3 transcription factor; liver fibrosis

1. Introduction

Liver fibrosis, a prevalent form of chronic liver disease, exhibits the hallmark of excessive hepatic extracellular matrix (ECM) deposition [1]. There are few efficacious clinical interventions for liver fibrosis, which may ultimately advance to hepatic cirrhosis, hepatic failure, or hepatocellular carcinoma (HCC). Hepatic stellate cell (HSC) is critical for the progression of liver fibrosis [2]. In the normal liver, quiescent HSCs usually serve as lipid-storing cells and the major cellular depot for vitamin A storage [3]. Upon liver damage, HSCs undergo activation and transdifferentiate into myofibroblast-like cells, a process that increases ECM synthesis and decreases ECM degradation, thereby inducing abnormal hepatic ECM deposition and culminating in liver fibrosis [4,5]. Efforts to regulate HSC activation thus represent a potential treatment strategy for liver fibrosis.

B-cell translocation gene 1 (BTG1), which belongs to the TOB/BTG family, has been reported to regulate cell cycle progression, suppress proliferative activity, and modulate cell differentiation [6]. In non-alcoholic fatty liver disease (NAFLD), BTG1 can inhibit triglyceride accumulation, thereby ameliorating disease progression [7,8]. Moreover, BTG1 acts as a potential tumor suppressor, and its downregulation is associated with hepatocarcinogenesis and poor clinical prognosis in HCC [9]. We previously reported that miR-301a-3p, which was bioinformatically predicted to target BTG1, promoted HSC activation [10]. These findings implied that the HSC-activating properties of miR-301a-3p may be mediated by BTG1. However,

BTG1's exact function in liver fibrogenesis and its regulatory pathways governing HSC activation remain unclear. Our study therefore aimed to clarify how BTG1 modulates HSC activation and proliferation to affect fibrotic disease progression in the liver.

The Janus kinase/signal transducer and activator of transcription (JAK/STAT) signaling pathways play an essential role in relaying cytokine signals from the cell membrane to the nucleus, thereby shaping multiple biological processes [11,12,13,14]. Prior investigations have indicated aberrant JAK2/STAT3 pathway activation in activated HSCs, driving liver fibrogenesis [11,12,15]. However, no previous reports have investigated whether BTG1 regulates HSC activation via the JAK2/STAT3 pathway. The present study aimed to clarify the functional mechanisms of BTG1 in modulating liver fibrosis and HSC activation, and further elucidate the key contribution of JAK2/STAT3 signaling to the regulatory effects of BTG1.

2. Materials and Methods

2.1 Cell Culture

HSC-T6 (CL-0116, Procell, Wuhan, China), an immortalized rat HSC line, was maintained at 37 °C with 5% CO_2 in high-glucose DMEM (Yuanpei Biotechnology, Shanghai, China) containing 10% fetal bovine serum (FBS; Gibco, Waltham, MA, USA), 1% penicillin and streptomycin (Beyotime, Shanghai, China). Cells at passages 3–8 were used for all cellular experiments in this study. To induce activation, HSC-T6 cells were incubated with 10 ng/mL of platelet-derived growth factor (PDGF-BB, 105-10, PrimeGene, Shanghai, China) for 48 h. Authentication of the cell line was performed using STR profiling, confirming the mycoplasma-free.

2.2 Animals

Six-week-old male Sprague-Dawley rats weighing 160–180 g were obtained from the Experimental Animal Center of Anhui Medical University (Anhui, China). Rats were randomly divided into four groups (n = 8 per group) by a random number table: control group, carbon tetrachloride (CCl_4) group, CCl_4 + adeno-associated virus (AAV)-control group, and CCl_4 + AAV-BTG1 group. Predefined animal exclusion criteria included abnormal weight, sickness, death, and unsuccessful fibrosis modeling. No animals were excluded throughout the study. For serum biochemical detection, hemolyzed or clotted serum samples were discarded; two serum samples from the CCl_4 group were excluded due to hemolysis, and six randomly selected serum samples per group were analyzed to balance sample sizes across cohorts. No samples were excluded from Western blotting, reverse transcription quantitative real-time polymerase chain reaction (RT-qPCR) or histological staining. Due to cost constraints, plate capacities, and time limitations, four randomly selected samples per group were analyzed for Western blotting and RT-qPCR, while three randomly selected liver tissue samples per group were used for histological evaluation. All remaining samples were retained as backups. To achieve blinding, all samples were labeled with unique coded identifiers. Group allocation, AAV injection, and CCl_4 administration were performed by an unblinded researcher due to procedural necessity. Subsequent tissue collection, histological staining, and immunohistochemical evaluation were completed by operators fully blinded to group assignments. Statistical analyses were completed by a fully blinded statistician, and unblinding was implemented only after all data processing was finalized. Rats were housed under controlled environmental conditions (20 ± 2 ℃) with a 12-h light-dark cycle. For liver-specific BTG1 overexpression, rats in the CCl_4 + AAV-BTG1 group received tail-vein injection of AAVs (HBAAV2/9-r-*Btg1*-3×flag-LUC, 1.6 × 10^{12} genome copies/mL, Hanheng Biotechnology, Shanghai, China). Rats in the CCl_4 + AAV-control group were injected with an empty AAV vector via the tail vein. Two weeks after AAV administration, liver fibrosis was induced by intraperitoneal injection of a 40% CCl_4-olive oil mixture (1 mL/kg), twice weekly for 8 weeks. Equal volumes of olive oil were intraperitoneally administered to the control rats at consistent intervals. 72 h after the last CCl_4 injection, all rats were anesthetized with isoflurane (3−4% induction concentration; 2−2.5% maintenance concentration). Blood and liver tissue samples were harvested after stable deep anesthesia was confirmed. After tissue collection, deeply anesthetized rats were placed into a sealed euthanasia chamber supplied with continuousand 100% CO_2 at a flow rate of 24 L/min. Following complete cessation of respiration, CO_2 exposure was maintained for a minimum of 10 min to confirm irreversible death via CO_2 inhalation euthanasia. The animal experiments were approved by the Animal Experimentation Ethics Committee of Anhui Medical University (No. LLSC20210990).

2.3 Small Interfering RNAs (siRNAs) and Transfection

BTG1-siRNA, negative control siRNA, and BTG1-overexpressing pcDNA3.1 vectors were supplied by Genepharma Co., Ltd (Suzhou, China). BTG1-siRNA: sense, 5′-UGGACUGAGCAGUCAAGAGTT-3′; antisense, 5′-CUCUUGACUGCUCAGUCCATT-3′. NC siRNA: sense, 5′-UUCUCCGAACGUGUCACGUTT-3′; antisense, 5′-ACGUGACACGUUCGGAGAATT-3′. pcDNA-BTG1: sense, 5′-TGGGCAGAACAAGCCCTTAAAAACT-3′; antisense, 5′-ACAATATGATGACTGTATCAGGTTAA-3′.

According to the manufacturer's directions, HSC-T6 cells plated at 5 × 10^5 cells/well were transfected with BTG1-siRNA, pcDNA-BTG1, or NC siRNA constructs using Lipofectamine 2000 (11668019, Invitrogen, USA). At 6 hours post-transfection, the cells were stimulated with 10 ng/mL PDGF-BB for 48 hours, then harvested.

2.4 JAK2 Inhibitor Treatment

Pretreatment with or without 3 μM ruxolitinib (a specific JAK2 inhibitor, S81142, Yuanye, Shanghai, China) for 6 h, cells transfected with BTG1-siRNA were incubated with 10 ng/mL PDGF-BB for 48 h. Cells transfected with negative control siRNA served as the control group.

2.5 Biochemical Analysis

Serum alanine aminotransferase (ALT) and aspartate aminotransferase (AST) levels were assayed utilizing commercial assay kits (105-000442-00 and 105-000443-00, Mindray, Shenzhen, China) with an automated biochemical analyzer (Mindray, Shenzhen, China). Following quality control and calibration, 10-fold diluted rat serum samples were loaded into the analyzer for precise measurement. Measurements were performed following the manufacturer's protocols.

2.6 Histopathology and Immunohistochemistry

4 μm-thick paraffin sections of liver tissue treated with 4% paraformaldehyde were stained with Masson's trichrome, hematoxylin and eosin (H&E), and Sirius red. To stain α-smooth muscle actin (α-SMA) and BTG1 immunohistochemically, paraffin liver sections were initially cultured with primary antibodies against α-SMA (1:500, AF1032, Affinity, USA) and BTG1 (1:500, 14879-1-AP, Proteintech, China) for 12 h at 4 °C, then incubated with biotinylated secondary antibody (bs-0295G-Bio, Bioss, Beijing, China) for 60 min at 25 °C. Diaminobenzidine (DAB) staining was used to view the sections, and hematoxylin was applied as a counterstain. Quantitative analysis was performed for five randomly selected fields per liver section.

2.7 Flow Cytometry Assay

The apoptotic rate of cells after BTG1 transfection was detected by an Annexin V-FITC/PI flow cytometry assay. Cells were harvested by EDTA-free trypsin 48 h after transfection, and processed according to the apoptosis detection kit's instructions (BB-4101, BestBio, Shanghai, China). 5 μL of Annexin V-FITC and 5 μL of propidium iodide (PI, 20 μg/mL) were employed to stain 4×10^5 cells for 15 min at 4°C in the dark. Subsequently, each sample with 10,000 cells was examined by a flow cytometer (Beckman Coulter, USA).

Gating strategy: Cell debris was excluded via FSC/SSC gating (P1), and single cells were further selected using FSC-A/FSC-H to remove cell doublets (P2). Fluorescence compensation was calibrated with single-stained controls to resolve spectral overlap between FITC and PI. With Annexin V-FITC on the x-axis and PI on the y-axis, quadrants were defined using unstained and single-stained controls: Q1 (necrotic cells, Annexin V−/PI+), Q2 (late apoptotic/necrotic cells, Annexin V+/PI+), Q3 (live cells, Annexin V−/PI−), Q4 (early apoptotic cells, Annexin V+/PI−). The total apoptotic rate was calculated as the sum of Q2 and Q4.

2.8 5-ethynyl-2'-deoxyuridine (EdU) Proliferation Assay

For evaluation of cell proliferation, HSC-T6 cells transfected with BTG1-siRNA or pcDNA-BTG1 as described above were incubated with a 10 μM EdU solution (C0078, Beyotime, Shanghai, China) at 37 °C for 2 h. After fixation in 4% paraformaldehyde and permeabilization in 0.3% Triton X-100, the cells were incubated with 0.5 mL of Click reaction solution for 30 min in the dark. Hoechst 33342 was used to stain cell nuclei. EdU-positive proliferating cells (red fluorescence) and nuclei (blue fluorescence) were observed and imaged by a fluorescence microscope (Leica, Germany).

2.9 Western Blotting

Protein from lysed samples was extracted using RIPA buffer containing PMSF (1:100). Proteins were separated using SDS-PAGE and transferred electrophoretically onto PVDF membranes (Millipore, Billerica, MA, USA). These membranes were incubated with primary antibodies overnight at 4 °C, followed by incubation with horseradish peroxidase-conjugated secondary antibodies (1:10,000, Zhongshan Jinqiao, China). Protein bands were visualized by ECL chemiluminescence, and the band intensity was quantitatively analyzed with ImageJ software (NIH, Bethesda, MD, USA). β-actin was used as the internal control. The primary antibodies utilized were specific for the following targets: α-SMA (AF1032), collagen I (AF7001), STAT3 (AF6294), p-STAT3 (AF3293), JAK2 (AF6022), p-JAK2 (AF3022) (1:1000, Affinity, USA), TNF-α (AF7014), cleaved caspase-3 (AF7022) (1:500, Affinity), β-actin (T0022, 1:2000, Affinity), BTG1 (14879-1-AP), Bcl-2 (26593-1-AP), Bax (50599-2-Ig), PCNA (10205-2-AP), Ki67 (84432-1-RR) and IL-6 (21865-1-AP) (1:1000, Proteintech, China). Representative blots are presented from three independent experiments.

2.10 RT-qPCR

The RNA extraction kit (AG21022, Accurate Biology, Hunan, China) was applied to extract total RNA. cDNA was synthesized by a reverse transcription kit (AG11705, Accurate Biology). RT-qPCR was conducted with the SYBR Green Premix Pro Taq HS qPCR kit (AG11701, Accurate Biology) with the real-time PCR detection system (Bio-Rad, USA). With β-actin as the internal normalization reference, the delta-delta threshold cycle ($2^{-\Delta\Delta Ct}$) approach was used to calculate relative gene expression levels. The primers used are provided in Table 1.

2.11 Statistical Analysis

All data analysis and figure generation were conducted using GraphPad Prism 8 (La Jolla, CA, USA). Multiple-group differences were performed using one-way ANOVA followed by Tukey's post-hoc test, while two-group differences were analyzed using Student's *t*-test. All data are presented as the mean ± standard deviation (SD).

Table 1. RT-qPCR primer sequences.

	Forward	Reverse
β-actin	GAGCGCAAGTACTCTGTGTG	CCTGCTTGCTGATCCACATC
α-SMA	GAGGGATCCTGACCCTGAAG	CCACGCGAAGCTCGTTATAG
collagen I	ACCTCAGGGTATTGCTGGAC	GACCAGGGAAGCCTCTTTCT
IL-6	GAGGATACCACTCCCAACAGACC	AAGTGCATCATCGTTGTTCATACA
TNF-α	ATGGGCTCCCTCTCATCAGTTCC	GCTCCTCCGCTTGGTGGTTTG
PCNA	TCACAAAAGCCACTCCACTGT	GCAACGCCTAAGATCCTTCC
Ki67	AACCATCATTGACCGCTCCTT	TTGACCTTCCCCATCAGGGT
Bax	CCAAGAAGCTGAGCGAGTGTCTC	CCAAGAAGCTGAGCGAGTGTCTC
Bcl-2	CAACATCGCCCTGTGGATGAC	CAACATCGCCCTGTGGATGAC
BTG1	CGTTGTATTCGCATCAACC	AGCCATCCTCTCCAATCC

α-SMA, α-smooth muscle actin; IL-6, interleukin-6; TNF-α, tumor necrosis factor-α; PCNA, proliferating cell nuclear antigen; BTG1, B-cell translocation gene 1; RT-qPCR, reverse transcription quantitative real-time polymerase chain reaction.

Representative images are shown. Statistical significance was set at $p < 0.05$.

Formal a priori power analysis was not conducted before animal assignment. The sample size (n = 8 per group) was determined based on our laboratory's previous experience with SD rat liver fibrosis models. Post-hoc power analysis was performed with α = 0.05 for two-tailed t-tests. For the primary comparisons (AAV-control vs. AAV-BTG1, control vs. CCl_4), the primary readouts (ALT, AST, α-SMA, Collagen I) exhibited Cohen's d values >4.58, and statistical power >0.99, confirming that n = 8 per group was sufficient to detect CCl_4-induced hepatic fibrosis and the therapeutic effect of BTG1.

3. Results

3.1 BTG1 Alleviates CCl_4-Induced Liver Fibrosis in Rats

To elucidate BTG1's function in liver fibrosis, an adeno-associated viral vector (AAV-*Btg1*) was employed to generate rats with liver-specific BTG1 overexpression. A 40% CCl_4 solution was injected intraperitoneally to establish the rat model of liver fibrosis. BTG1 was successfully overexpressed in the livers of CCl_4+AAV-BTG1 group rats relative to CCl_4-treated rats, as demonstrated by Western blotting and RT-qPCR (Fig. 1A,B). To investigate whether BTG1 alleviates CCl_4-induced liver injury in this experimental system, serum ALT and AST levels of rats following an 8-week treatment with 40% CCl_4 were measured. Rats treated with CCl_4 exhibited markedly higher serum ALT and AST levels than the normal controls, indicating the hepatic function impairment induced by CCl_4. AAV-mediated BTG1 overexpression significantly attenuated CCl_4-induced increases in serum ALT and AST levels, indicating alleviation of liver injury (Fig. 1C,D). Hepatic histopathological changes and collagen deposition were evaluated following the staining methods detailed in Section 2.6. As illustrated in Fig. 1E, compared with the normal controls, livers from CCl_4-treated rats displayed disordered hepatic lobular structures, lipid degeneration, inflammatory cell infiltration, collagen deposition, and fibrous tissue proliferation in the portal area, thus confirming the successful induction of experimental rat liver fibrosis. In rats from the CCl_4+AAV-BTG1 group, liver fibrosis was markedly attenuated, as evidenced by restored hepatic lobular architecture, reduced hepatic steatosis, decreased inflammatory cell infiltration and collagen deposition, and reduced portal fibrous tissue hyperplasia. As assessed by immunohistochemistry, α-SMA expressionwas increased in the liver tissue of CCl_4-treated rats relative to the normal controls, whereas it was decreased in CCl_4+AAV-BTG1 rats compared with the CCl_4-treated rats (Fig. 1F). The expression of IL-6, TNF-α, α-SMA, and collagen I in rat liver tissue was measured. CCl_4 treatment induced a marked upregulation of the expression of these markers compared with the normal controls, which was significantly downregulated by AAV-mediated BTG1 overexpression (Fig. 1G,H). These findings indicate that BTG1 overexpression alleviates CCl_4-induced liver damage and ameliorates liver fibrosis in rats.

3.2 BTG1 is Downregulated in Activated HSCs

The expression of BTG1, fibrotic markers (α-SMA and collagen I), IL-6, and TNF-α was analyzed in PDGF-BB-induced activated HSC-T6 cells by Western blotting and RT-qPCR. Compared with untreated controls, α-SMA, collagen I, IL-6, and TNF-α expression was markedly upregulated in the PDGF-BB-treated cells with a corresponding significant decline in BTG1 protein and mRNA expression (Fig. 2). PDGF-BB was thus found to induce HSC-T6 cell activation, while reducing BTG1 expression in activated HSCs.

3.3 Liposome-Mediated Transfection Results in BTG1 Overexpression or Knockdown in HSC-T6 Cells

As illustrated in Fig. 3A,B, Western blotting and RT-qPCR analyses demonstrated that BTG1 expression was markedly downregulated in BTG1-siRNA-

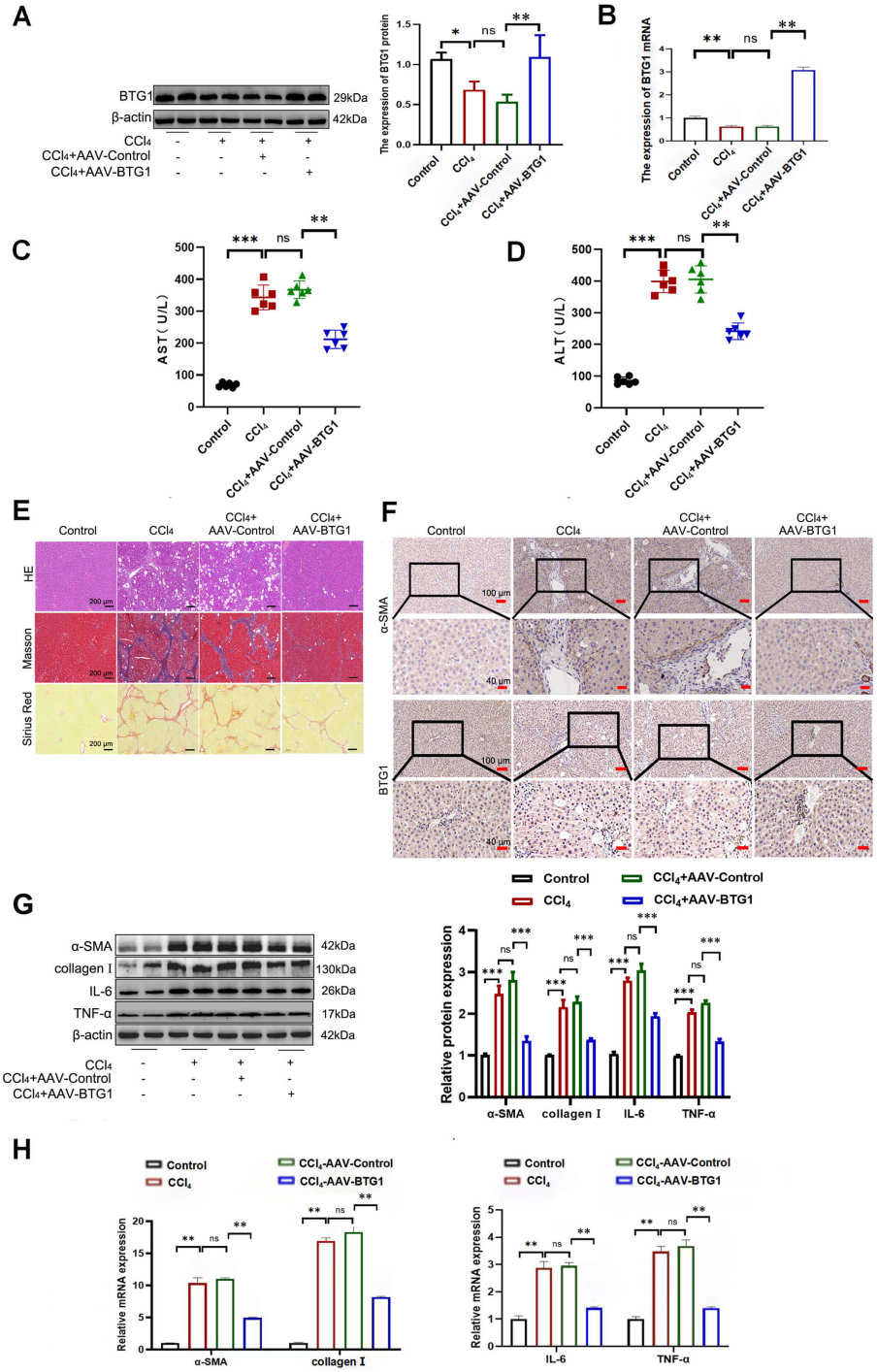

Fig. 1. BTG1 alleviates CCl_4-induced liver fibrosis in rats. (A,B) Representative western blotting images (2 representative replicates from n = 4 per group) and RT-qPCR quantification of BTG1 expression in rat liver tissues (n = 4). (C,D) Serum levels of ALT and AST were measured by biochemical analysis (n = 6). (E) Representative H&E, Masson's trichrome, and Sirius red staining of liver sections from each group (scale bar: 200 μm; n = 3). (F) Representative immunohistochemistry images of α-SMA and BTG1 expression in liver tissue (scale bars: 100 μm (original images), 40 μm (magnified images); n = 3). (G,H) Representative western blotting images (2 representative replicates from n = 4 per group) and RT-qPCR quantification of α-SMA, collagen I, IL-6, and TNF-α protein and mRNA levels in liver tissue (n = 4). Analyzed by one-way ANOVA. *$p < 0.05$, **$p < 0.01$, ***$p < 0.001$; ns, no significant difference. CCl_4, carbon tetrachloride; RT-qPCR, reverse transcription quantitative real-time polymerase chain reaction; ALT, alanine aminotransferase; AST, aspartate aminotransferase; H&E, hematoxylin and eosin; ANOVA, analysis of variance.

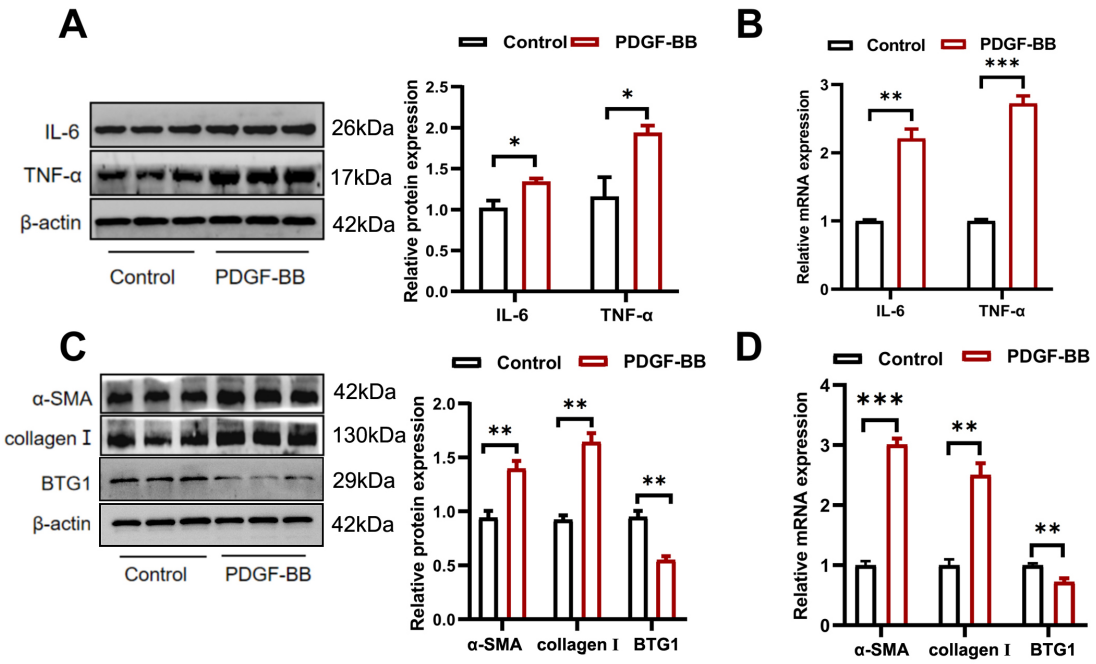

Fig. 2. BTG1 expression is downregulated in activated HSCs. Western blotting and RT-qPCR were performed to detect the expression of IL-6 and TNF-α (A,B), as well as α-SMA, collagen I, and BTG1 (C,D), in HSC-T6 cells following PDGF-BB treatment (10 ng/mL, 48 h). Student's *t*-test was applied for statistical analysis (n = 3). *$p < 0.05$, **$p < 0.01$, ***$p < 0.001$. HSCs, hepatic stellate cells; PDGF-BB, platelet-derived growth factor-BB.

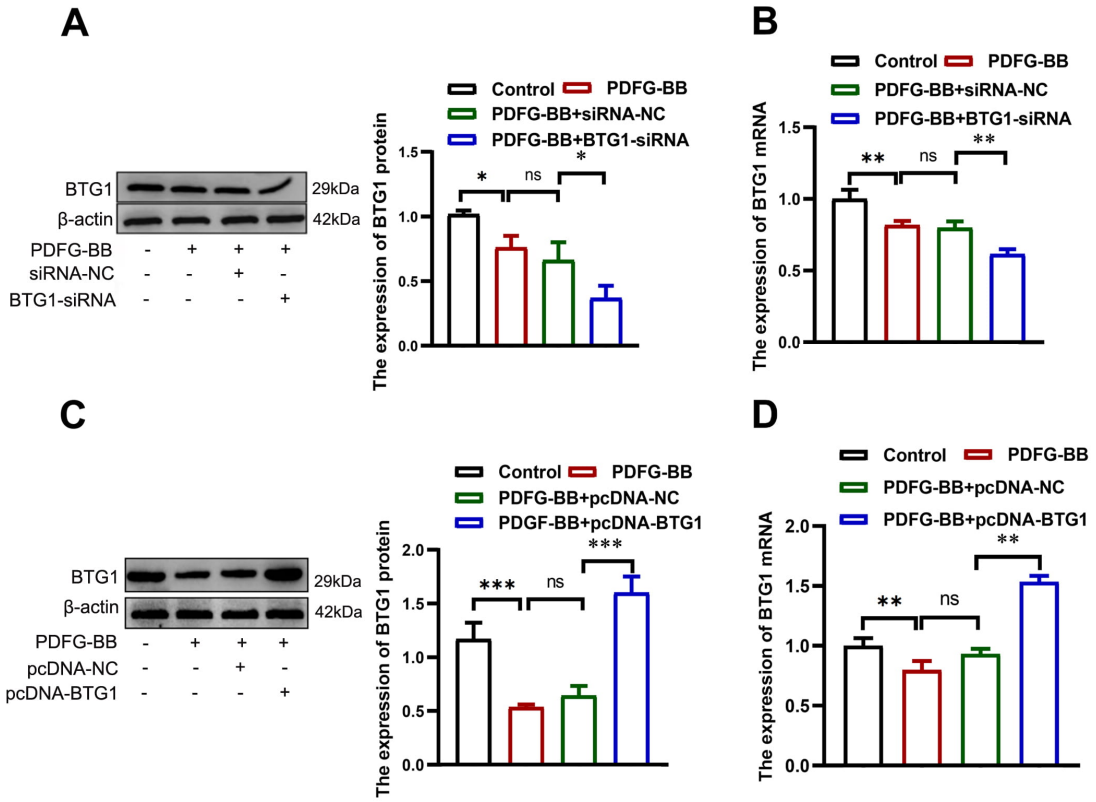

Fig. 3. Liposome-mediated transfection results in BTG1 knockdown or overexpression in HSC-T6 cells. BTG1 expression was determined by Western blotting and RT-qPCR in HSC-T6 cells following BTG1 knockdown (A,B) or overexpression (C,D). A representative Western blotting image is shown. Quantitative data were analyzed by one-way ANOVA (n = 3). *$p < 0.05$, **$p < 0.01$, ***$p < 0.001$; ns, no significant difference.

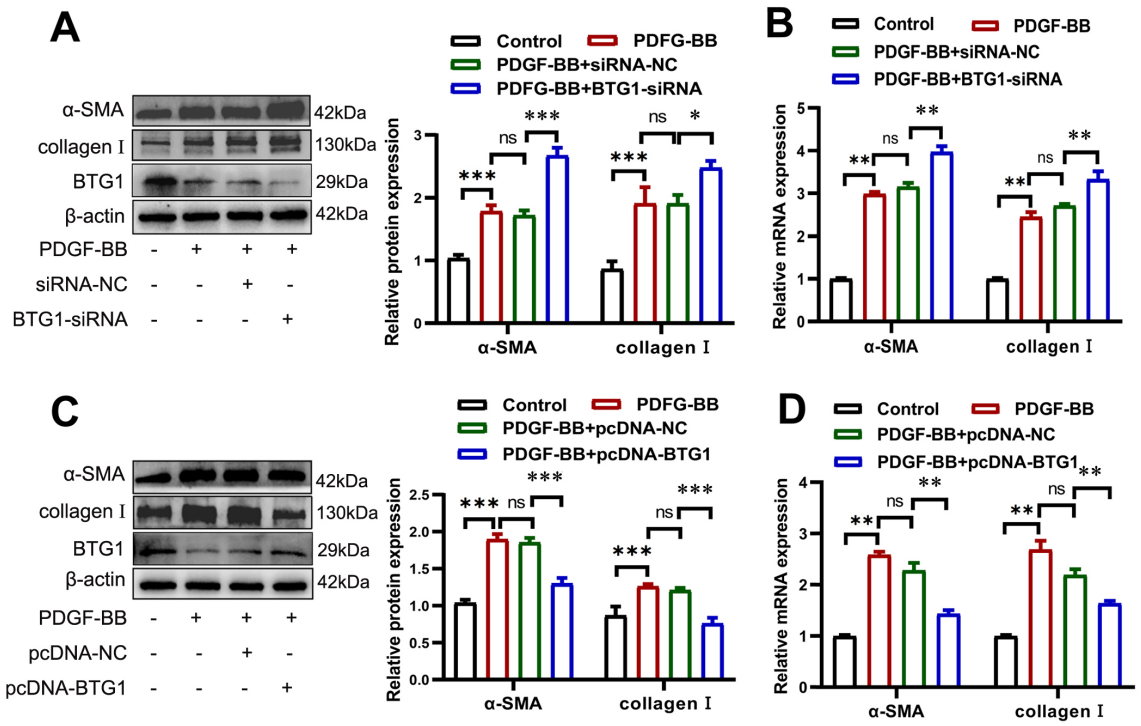

Fig. 4. BTG1 modulates α-SMA and collagen I expression in HSC-T6 cells. HSC-T6 cells were transfected with BTG1-siRNA (A,B) or pcDNA-BTG1 (C,D), then stimulated with PDGF-BB. The levels of α-SMA and collagen I were detected using Western blotting and RT-qPCR. A representative Western blotting image is shown. Quantitative data were analyzed by one-way ANOVA (n = 3). *$p < 0.05$, **$p < 0.01$, ***$p < 0.001$; ns, no significant difference.

transfected HSC-T6 cells, whereas transfection with BTG1-overexpression plasmids (pcDNA-BTG1) significantly upregulated BTG1 expression in HSC-T6 cells (Fig. 3C,D). These findings lay the foundation for subsequent functional studies of BTG1 in HSC-T6 cells.

3.4 BTG1 Modulates PDGF-BB-Induced HSC-T6 Cell Activation

The regulatory effects of BTG1 on fibrotic marker expression were analyzed. siRNA-mediated BTG1 knockdown significantly upregulated α-SMA and collagen I expression in PDGF-BB-treated HSC-T6 cells (Fig. 4A,B), whereas BTG1 overexpression led to the marked downregulation of both fibrotic markers (Fig. 4C,D). These results indicate that BTG1 inhibits fibrotic marker expression in activated HSCs, indicating that it functions as an antifibrotic gene in liver fibrosis.

3.5 BTG1 Modulates PDGF-BB-Induced Inflammatory Response in HSC-T6 Cells

IL-6 and TNF-α are critical mediators of hepatic inflammation and promote HSC activation and liver fibrosis progression [16]. The expression of IL-6 and TNF-α was determined in HSC-T6 cells. As shown in Fig. 5A,B, BTG1 knockdown significantly elevated IL-6 and TNF-α expression. Conversely, BTG1 overexpression markedly downregulated the expression of both cytokines (Fig. 5C,D). Thus, the observations above suggest that BTG1 alleviates hepatic inflammatory response.

3.6 BTG1 Regulates PDGF-BB-Induced Proliferation and Apoptosis in HSC-T6 Cells

To clarify BTG1's roles as a key mediator in the proliferation and apoptosis of activated HSCs, BTG1 was silenced or overexpressed in HSC-T6 cells, prior to PDGF-BB treatment. The EdU proliferation assay suggested that siRNA-mediated BTG1 knockdown promoted the proliferation of PDGF-BB-treated HSC-T6 cells (Fig. 6A). Correspondingly, quantitative western blotting and RT-qPCR analyses revealed marked upregulation of the key proliferation markers Ki67 and PCNA upon BTG1 silencing (Fig. 6C,D). Moreover, representative EdU staining showed fewer PDGF-BB-induced EdU-positive cells following BTG1 overexpression (Fig. 6B), accompanied by significant downregulation of Ki67 and PCNA (Fig. 6E,F).

To explore a potential link between the antiproliferative effect of BTG1 and cellular apoptosis, Annexin V-FITC/PI flow cytometry staining was performed. The results showed that siRNA-mediated BTG1 silencing significantly decreased the apoptotic rate of PDGF-BB-treated HSC-T6 cells from 22.05 ± 1.62% to 12.86 ± 1.25% (Fig. 7A). In contrast, BTG1 overexpression significantly increased the apoptotic rate of PDGF-BB-treated HSC-T6 cells from 20.99 ± 1.83% to 27.66 ± 1.06% (Fig.

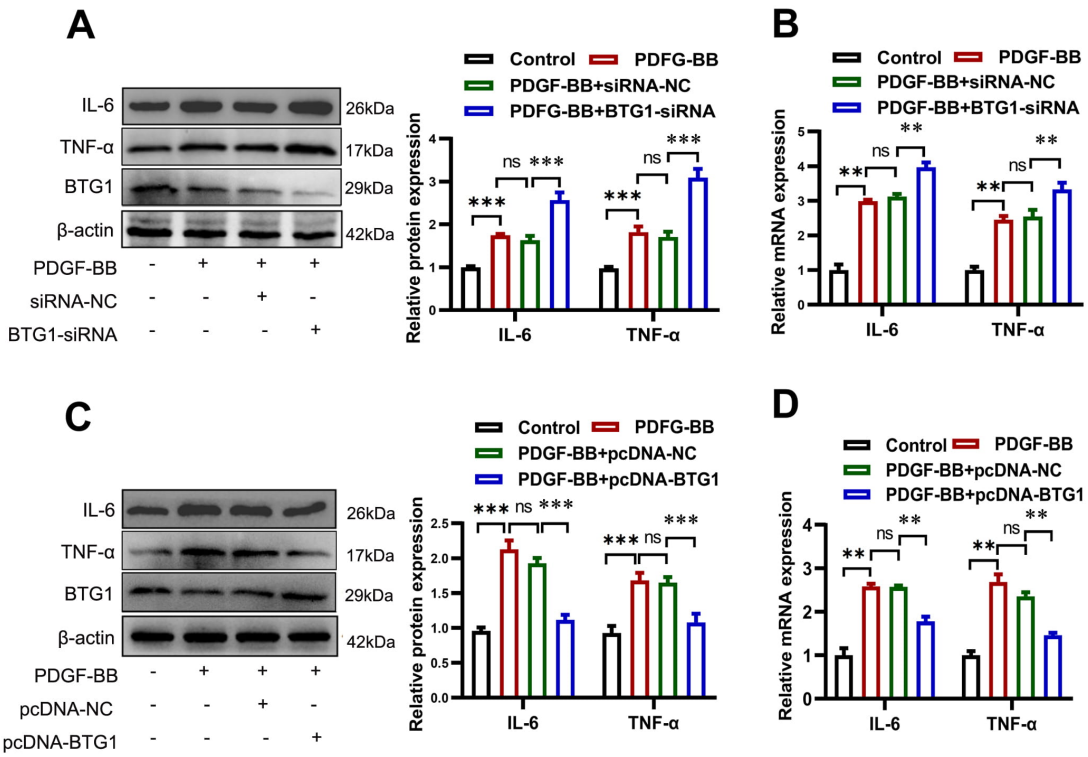

Fig. 5. BTG1 modulates inflammatory response in HSC-T6 cells. The levels of IL-6 and TNF-α protein and mRNA were determined using Western blotting and RT-qPCR in HSC-T6 cells with BTG1-siRNA (A,B) or pcDNA-BTG1 (C,D) following PDGF-BB treatment. A representative Western blotting image is shown. Quantitative data were analyzed by one-way ANOVA (n = 3). $^{**}p < 0.01$, $^{***}p < 0.001$; ns, no significant difference.

7B). As shown in Fig. 7C,D, BTG1 silencing resulted in a significant downregulation of the pro-apoptotic mediators Bax and cleaved caspase-3, while causing the upregulation of the anti-apoptotic protein Bcl-2 in activated HSC-T6 cells. Bcl-2 and Bax showed consistent expression changes at protein and mRNA levels, while cleaved caspase-3 was only assessed at the protein level. Conversely, BTG1 overexpression exerted the opposite effect on the PDGF-induced expression of these apoptotic regulators (Fig. 7E,F). These results demonstrate that BTG1 inhibits the proliferation of activated HSCs and promotes apoptosis.

3.7 BTG1 Suppresses JAK2/STAT3 Pathway Signaling in Activated HSCs

Compelling evidence indicates that aberrant activation of the JAK2/STAT3 signaling pathway represents a major molecular event mediating HSC activation [13]. To elucidate the potential regulatory mechanism underlying BTG1-mediated anti-fibrotic action, the protein levels of p-JAK2, total JAK2, p-STAT3, and total STAT3 were measured in activated HSCs. Western blotting showed that PDGF-BB treatment induced a marked increase in p-JAK2 and p-STAT3 levels in HSC-T6 cells, whereas total protein expression of JAK2 and STAT3 remained unchanged (Fig. 8A,B). Next, BTG1-silenced or BTG1-overexpressing HSC-T6 cells were employed to evaluate the key regulatory effect of BTG1 on the JAK2/STAT3 signaling pathway. siRNA-mediated BTG1 knockdown markedly enhanced PDGF-BB-induced JAK2 and STAT3 phosphorylation, whereas BTG1 overexpression exerted the opposite effect, reducing p-JAK2 and p-STAT3 levels in HSC-T6 cells (Fig. 8A,B). Subsequently, the JAK inhibitor ruxolitinib was used to block JAK2/STAT3 signaling in HSCs. Ruxolitinib pretreatment effectively reversed the BTG1-silencing-induced hyperphosphorylation of JAK2 and STAT3 (Fig. 8C), and attenuated the upregulation of key myofibroblast activation markers (α-SMA, collagen I) and inflammatory cytokines (IL-6, TNF-α) (Fig. 8D). The data indicate that BTG1 inhibits HSC activation by negatively regulating the JAK2/STAT3 pathway.

4. Discussion

Liver fibrosis is pathologically characterized by hepatic architectural alterations that arise in response to chronic injury, which involve persistent HSC activation, hepatocyte damage and regeneration, and excessive ECM deposition [17,18,19]. Liver fibrosis has a complex pathogenesis that is driven by multiple factors, including hepatotoxic stimuli, hepatic metabolic dysfunction, and cholestasis, which collectively induce hepatocyte injury and immune cell infiltration, thereby promoting the differentiation of HSCs into

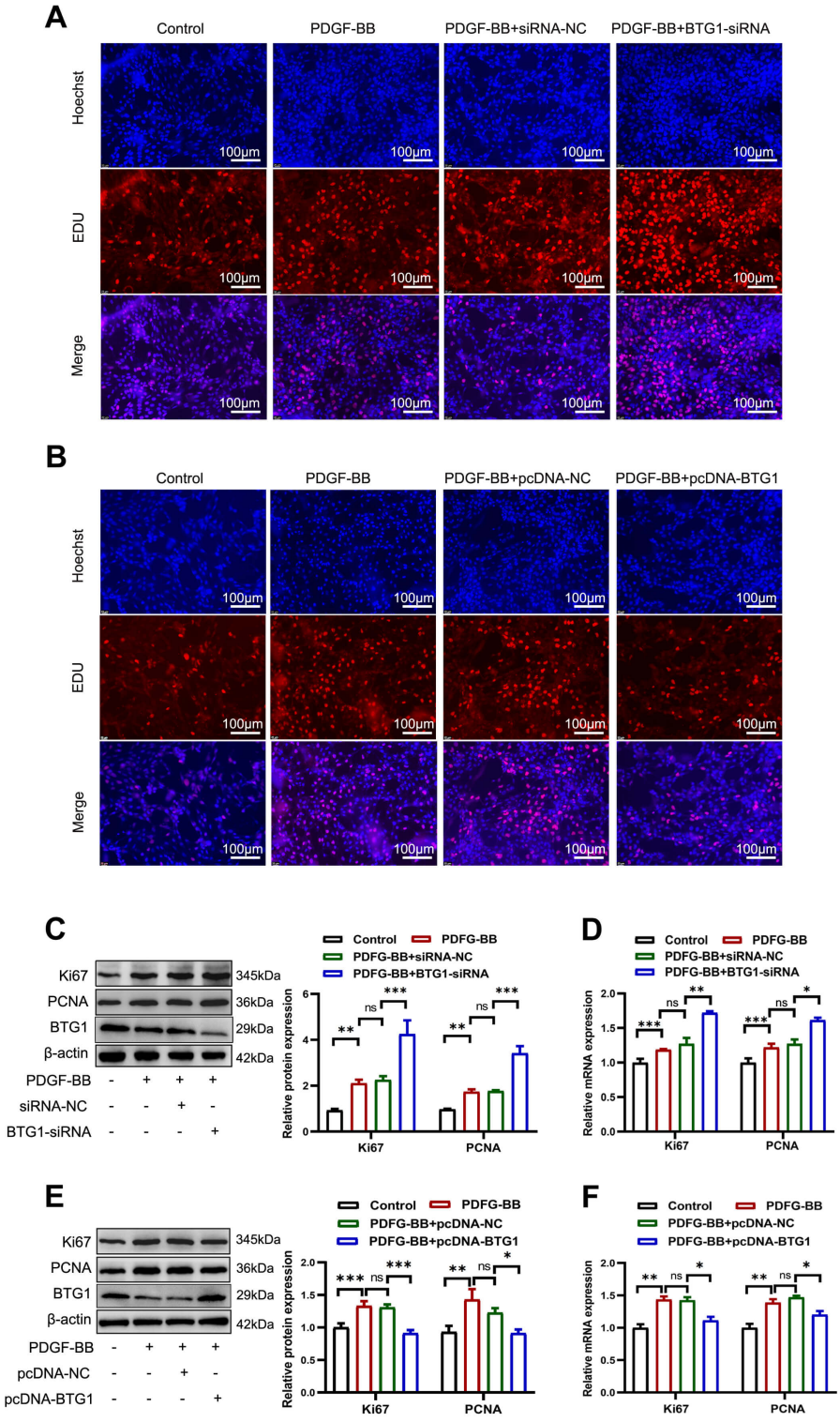

Fig. 6. BTG1 regulates the PDGF-BB-induced proliferation in HSC-T6 cells. (A,B) An EdU proliferation assay was utilized to detect BTG1's effect on activated HSC-T6 cell proliferation. Nuclei were counterstained with Hoechst. Representative fluorescence microscopy images are shown (scale bar: 100 μm). (C–F) The levels of Ki67 and PCNA protein and mRNA were determined using Western blotting and RT-qPCR in PDGF-BB-treated HSC-T6 cells transfected with BTG1-siRNA (C,D) or pcDNA-BTG1 (E,F). A representative Western blotting image is shown. Quantitative data were analyzed by one-way ANOVA (n = 3). *$p < 0.05$, **$p < 0.01$, ***$p < 0.001$; ns, no significant difference.

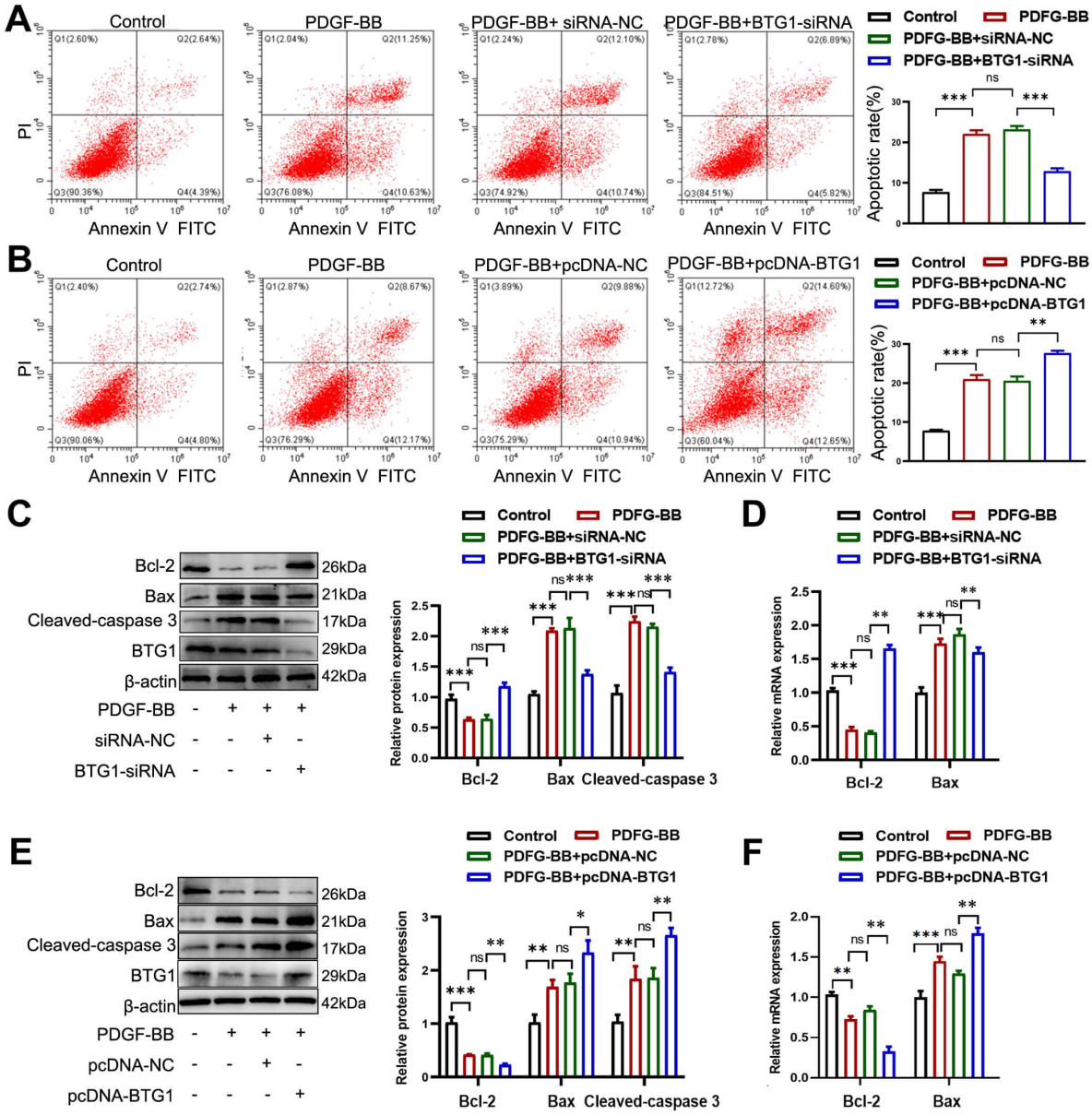

Fig. 7. BTG1 regulates the PDGF-BB-induced apoptosis in HSC-T6 cells. (A,B) An Annexin V-FITC/PI flow cytometry assay was applied to analyze the apoptotic rate of HSC-T6 cells. In the presented scatterplots, quadrant Q1 corresponds to necrotic cells (Annexin V−/PI+), quadrant Q2 corresponds to late apoptotic cells (Annexin V+/PI+), quadrant Q3 corresponds to live cells (Annexin V−/PI−), and quadrant Q4 corresponds to early apoptotic cells (Annexin V+/PI−). The accompanying bar graphs summarize the quantified percentage of early and late apoptotic cells. (C–F) The expression of apoptosis-associated proteins was assessed in HSC-T6 cells transfected with BTG1-siRNA or pcDNA-BTG1. Protein levels were measured by Western blotting, and mRNA levels of Bcl-2 and Bax were quantified by RT-qPCR. A representative Western blotting image is shown. Quantitative data were analyzed by one-way ANOVA (n = 3). *p < 0.05, **p < 0.01, ***p < 0.001; ns, no significant difference.

myofibroblasts [20,21,22,23]. Activated HSCs produce α-SMA, collagen, and other ECM components, leading to excessive ECM accumulation and subsequent progression to liver fibrosis and HCC [24]. Multiple cytokines and signaling pathways interact to regulate HSC activation, including those stimulated by TGF-β1, PDGF, and VEGF, and HSC activation is additionally responsive to oxidative stress and endoplasmic reticulum stress [25,26,27]. The elucidation of the regulatory mechanisms underlying HSC activation is thus crucial to guide the formulation of therapeutic approaches suitable for liver fibrosis.

BTG1, an anti-proliferative factor, is essential for governing cell proliferation, differentiation, and apoptosis [28,29]. Emerging evidence has linked the dysregulated BTG1 expression to the pathogenesis of certain diseases. Existing literature has confirmed that BTG1 upregulation

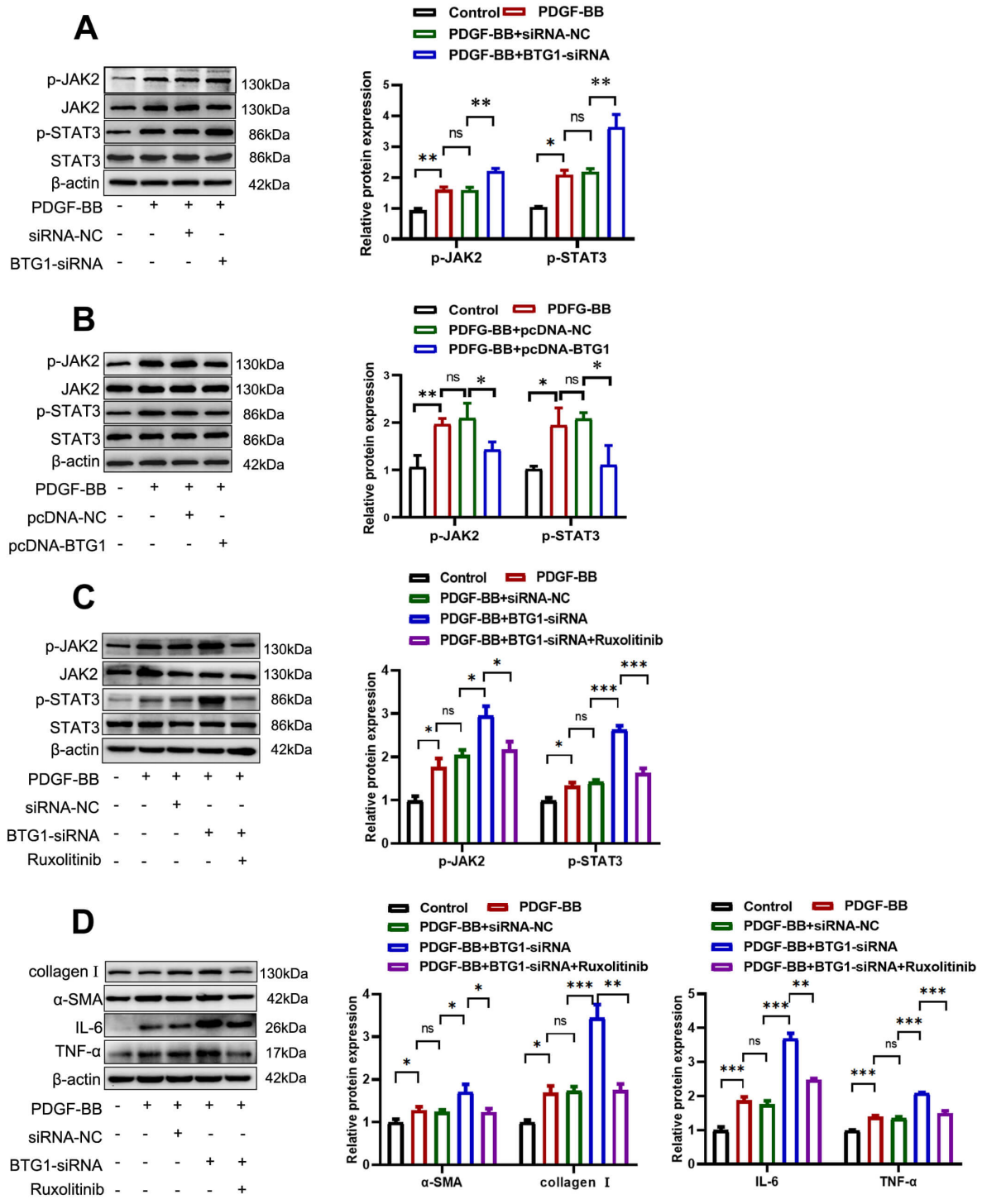

Fig. 8. BTG1 regulates the JAK2/STAT3 pathway activation in HSC-T6 cells. (A,B) The phosphorylated and total JAK2 and STAT3 protein levels were determined via Western blotting in HSC-T6 cells; total protein expression remained unchanged. (C,D) The protein levels of p-JAK2, p-STAT3, JAK2, STAT3, collagen I, α-SMA, IL-6, and TNF-α in BTG1-silenced HSC-T6 cells pretreated with or without ruxolitinib (3 μM, 6 h) were detected by Western blotting. A representative Western blotting image is shown. Quantitative data were analyzed by one-way ANOVA (n = 3). *$p < 0.05$, **$p < 0.01$, ***$p < 0.001$; ns, no significant difference.

significantly suppresses the proliferation of malignant cells in lung cancer and breast cancer [30,31]. BTG1 overexpression reportedly reduces the levels of key cell cycle checkpoint proteins, suggesting that it suppresses cell cycle progression [32]. Furthermore, BTG1 induces apoptosis in prostate cancer cells and vascular smooth muscle cells by reducing the levels of Bcl-2 [33,34]. Notably, BTG1 alleviates hepatic steatosis in NAFLD by inhibiting intra-

hepatic triglyceride accumulation and adipogenesis-related gene expression [7]. Despite these advances, the functional importance of BTG1 in HSCs and liver fibrosis remains unexplored. Given its anti-proliferative properties and regulatory effects on metabolic pathways, we hypothesized that BTG1 may modulate HSC activation and proliferation in liver fibrosis, prompting this study to investigate BTG1 mechanistic functions in the pathogenesis of liver fibrosis.

The CCl_4-induced liver fibrosis rat model is well-validated, with pathological features similar to human chemical-induced liver fibrosis. As previously reported, liver injury is correlated with the downregulation of BTG1 protein levels in the livers of HCC patients and NAFLD mice [7]. Our study demonstrated significantly downregulated BTG1 expression in liver tissues and increased serum ALT/AST activities in CCl_4-induced fibrotic rats. Notably, hepatic-specific overexpression of BTG1 significantly reduced serum ALT/AST levels compared with the CCl_4-treated group, indicating its hepatoprotective effect against chemical-induced liver injury. Histopathological analysis revealed that BTG1 overexpression ameliorated hepatic tissue architecture disorder and alleviated collagen deposition. Western blotting illustrated that BTG1 overexpression markedly downregulated the protein levels of α-SMA, collagen I, IL-6, and TNF-α in liver tissues. Since inflammatory factors promote HSC activation to accelerate fibrosis [17], BTG1 may exert anti-fibrotic effects through attenuating inflammatory responses. *In vitro*, BTG1 was downregulated in activated HSC-T6 cells. BTG1 knockdown induced HSC activation and proliferation, inhibited HSC apoptosis, and upregulated fibrosis- and inflammation-associated markers, while BTG1 overexpression exerted the opposite effects. These outcomes confirm that BTG1 is a critical inhibitor of HSC activation, exerting an anti-fibrotic effect in the pathogenesis of liver fibrosis.

PDGF, which serves as a pro-proliferative factor for HSCs, activates multiple signaling pathways, especially the MAPK, PI3K, and JAK pathways, by binding to its receptor (PDGF-βR), thereby driving fibrogenic responses [35,36]. The JAK/STAT3 signaling axis, in particular, has been firmly established as a critical mediator of HSC activation. Notably, functional divergence in JAK/STAT3 signaling has been reported depending on the specific kinases involved. While JAK1/STAT3 activation exerts cytoprotective effects in HSCs, the JAK2/STAT3 axis predominantly mediates profibrotic responses [37,38]. Upon PDGF stimulation, receptor dimerization triggers a sequential phosphorylation cascade: JAK2 undergoes autophosphorylation and subsequently phosphorylates STAT3, which promotes STAT3 dimerization and nuclear translocation. The activated STAT3 complex subsequently binds to promoter regions of pro-fibrotic genes (e.g., α-SMA), thereby facilitating HSC activation [39]. The present study revealed that BTG1 knockdown markedly increased JAK2 and STAT3 phosphorylation levels in activated HSCs, accompanied by upregulation of α-SMA, collagen I, IL-6, and TNF-α. Conversely, BTG1 overexpression exhibited the opposite effects by suppressing JAK2/STAT3 pathway activation and its downstream fibro-inflammatory targets. To confirm BTG1's regulatory function in the JAK2/STAT3 pathway, the selective JAK2 inhibitor ruxolitinib was applied in BTG1-silenced HSCs. The results demonstrated that the JAK2 inhibitor significantly attenuated the BTG1 knockdown-induced hyperphosphorylation of JAK2 and STAT3, along with the upregulation of fibrotic markers and inflammatory cytokines. Collectively, these results confirm that BTG1 suppresses HSC activation primarily through inhibition of the JAK2/STAT3 pathway. Alongside our prior findings [10], these results establish a functional regulatory axis that governs HSC activation in the form of the miR-301a-3p/BTG1/JAK2-STAT3 pathway. Meanwhile, the highlight of BTG1 as a critical mediator that links non-coding RNA regulation to the JAK2/STAT3 signaling cascade during liver fibrosis, thereby providing a promising target for therapeutic intervention in this pathological condition.

While the above findings are promising, this study has several limitations. Although our current data confirmed that BTG1 negatively regulates the JAK2/STAT3 pathway by altering the phosphorylation levels of JAK2 and STAT3, thereby inhibiting HSC activation and hepatic inflammatory infiltration, the detailed molecular mechanisms by which BTG1 modulates JAK2/STAT3 phosphorylation are yet to be elucidated. We will elucidate the underlying mechanism in subsequent studies to determine whether BTG1 regulates this pathway through direct physical interaction with JAK2/STAT3 or by modulating the activity of relevant phosphatases. Furthermore, the present study primarily relied on HSC models and rat liver fibrosis models, which, despite their extensive use, cannot accurately recapitulate the intricate pathological features and progression of human liver fibrosis. Therefore, additional studies employing human liver samples and clinical investigations are warranted to systematically verify the expression and regulatory mechanism of BTG1 during different stages of human liver fibrosis, thereby providing more reliable experimental and clinical evidence for its translational potential in the therapeutic intervention of liver fibrosis.

5. Conclusion

These results demonstrate that BTG1 can significantly suppress the development of CCl_4-induced liver fibrosis in rats. Furthermore, *in vitro* data indicate that BTG1 modulates the PDGF-BB-induced activation, proliferation, apoptosis, and inflammatory responses of HSCs. Mechanistically, these biological effects of BTG1 are achieved by inhibiting the activation of the JAK2/STAT3 signaling pathway. Collectively, the present study demonstrates that BTG1 acts as a critical regulator of key cellular events underlying liver fibrosis progression, suggesting that target-

ing BTG1 to inhibit HSC activation may provide a potential strategy for anti-fibrotic interventions.

Abbreviations

AAV, adeno-associated virus; ALT, alanine aminotransferase; AST, aspartate aminotransferase; BTG1, B-cell translocation gene 1; CCl_4, carbon tetrachloride; ECM, extracellular matrix; HCC, hepatocellular carcinoma; H&E, hematoxylin and eosin; HSCs, hepatic stellate cells; IL-6, interleukin-6; JAK/STAT, Janus kinase/signal transducer and activator of transcription; NAFLD, non-alcoholic fatty liver disease; PDGF-BB, platelet-derived growth factor-BB; RT-qPCR, reverse transcription quantitative real-time polymerase chain reaction; TNF-α, tumor necrosis factor-α; α-SMA, α-smooth muscle actin.

Availability of Data and Materials

The datasets involved in the current study are available from the corresponding authors upon reasonable request.

Author Contributions

WL: Conceptualization, Methodology, Data Curation, Visualization, Writing—Original Draft, Supervision, Validation. ZA and ML: Methodology, Data Curation, Software, Visualization. JK: Methodology, Data Curation, Visualization. LW: Data Curation, Software, Visualization. XF: Data Curation, Software, Validation, Writing—Review & Editing. FW: Design, Writing—Review & Editing, Supervision, Funding acquisition. All authors contributed to editorial changes in the manuscript. All authors read and approved the final manuscript. All authors have participated sufficiently in the work and agreed to be accountable for all aspects of the study.

Ethics Approval and Consent to Participate

The animal experiments were approved by the Animal Experimentation Ethics Committee of Anhui Medical University (No. LLSC20210990), the study was carried out in accordance with the ARRIVE guidelines, and all the procedures were performed in accordance with the NIH Guide for the Care and Use of Laboratory Animals.

Acknowledgment

We appreciate FigDraw platform for providing FigDraw 2.0 software to prepare the graphical abstract of this manuscript.

Funding

This project was supported by grants from the Natural Science Research Project of Anhui Educational Committee (2022AH050767, 2023AH050676), National Natural Science Foundation of China (82470659), Basic and Clinical Cooperative Research Promotion Program of Anhui Medical University-Incubation Project for The Third Affiliated Hospital (2023sfy011), Research Project of the Provincial Entrepreneurship Research Institute of Anhui Medical University (Document No. Chuangxin Fa (2025) No. 6) and Pharmaceutical Innovation Fund of Anhui Medical University (YXCX202103).

Conflicts of Interest

The authors declare no conflicts of interest.

Supplementary Material

Supplementary material associated with this article can be found, in the online version, at https://doi.org/10.31083/FBL51017.

References

[1] Kisseleva T, Brenner D. Molecular and cellular mechanisms of liver fibrosis and its regression. Nature Reviews. Gastroenterology & Hepatology. 2021; 18: 151–166. https://doi.org/10.1038/s41575-020-00372-7

[2] Akkız H, Gieseler RK, Canbay A. Liver Fibrosis: From Basic Science towards Clinical Progress, Focusing on the Central Role of Hepatic Stellate Cells. International Journal of Molecular Sciences. 2024; 25: 7873. https://doi.org/10.3390/ijms25147873

[3] Blaner WS, O'Byrne SM, Wongsiriroj N, Kluwe J, D'Ambrosio DM, Jiang H, et al. Hepatic stellate cell lipid droplets: a specialized lipid droplet for retinoid storage. Biochimica et Biophysica Acta. 2009; 1791: 467–473. https://doi.org/10.1016/j.bbalip.2008.11.001

[4] Ezhilarasan D. Mitochondria: A critical hub for hepatic stellate cells activation during chronic liver diseases. Hepatobiliary & Pancreatic Diseases International : HBPD INT. 2021; 20: 315–322. https://doi.org/10.1016/j.hbpd.2021.04.010

[5] Kuchay MS, Choudhary NS, Mishra SK. Pathophysiological mechanisms underlying MAFLD. Diabetes & Metabolic Syndrome. 2020; 14: 1875–1887. https://doi.org/10.1016/j.dsx.2020.09.026

[6] Chen XQ, Meng FQ, Xiong H, Wang YL, Tang WH, Zou YM. Identification of BTG1 Status in Solid Cancer for Future Researches Using a System Review and Meta-analysis. Current Medical Science. 2020; 40: 85–94. https://doi.org/10.1007/s11596-020-2150-z

[7] Xiao F, Deng J, Guo Y, Niu Y, Yuan F, Yu J, et al. BTG1 ameliorates liver steatosis by decreasing stearoyl-CoA desaturase 1 (SCD1) abundance and altering hepatic lipid metabolism. Science Signaling. 2016; 9: ra50. https://doi.org/10.1126/scisignal.aad8581

[8] Zhou X, Yuan Y, Teng F, Li K, Luo S, Zhang P, et al. Obesity-induced upregulation of microRNA-183-5p promotes hepatic triglyceride accumulation by targeting the B-cell translocation gene 1. Life Sciences. 2021; 268: 119011. https://doi.org/10.1016/j.lfs.2020.119011

[9] Kanda M, Sugimoto H, Nomoto S, Oya H, Hibino S, Shimizu D, et al. B-cell translocation gene 1 serves as a novel prognostic indicator of hepatocellular carcinoma. International Journal of Oncology. 2015; 46: 641–648. https://doi.org/10.3892/ijo.2014.2762

[10] Luan SH, Yang YQ, Ye MP, Liu H, Rao QF, Kong JL, et al. ASIC1a promotes hepatic stellate cell activation through the exosomal miR-301a-3p/BTG1 pathway. International Journal of Biological Macromolecules. 2022; 211: 128–139. https://doi.org/10.1016/j.ijbiomac.2022.05.041

[11] Xin P, Xu X, Deng C, Liu S, Wang Y, Zhou X, et al. The role

of JAK/STAT signaling pathway and its inhibitors in diseases. International Immunopharmacology. 2020; 80: 106210. https://doi.org/10.1016/j.intimp.2020.106210

[12] Liu J, Wang F, Luo F. The Role of JAK/STAT Pathway in Fibrotic Diseases: Molecular and Cellular Mechanisms. Biomolecules. 2023; 13: 119. https://doi.org/10.3390/biom13010119

[13] Fortelny N, Farlik M, Fife V, Gorki AD, Lassnig C, Maurer B, et al. JAK-STAT signaling maintains homeostasis in T cells and macrophages. Nature Immunology. 2024; 25: 847–859. https://doi.org/10.1038/s41590-024-01804-1

[14] Erdogan F, Radu TB, Orlova A, Qadree AK, de Araujo ED, Israelian J, et al. JAK-STAT core cancer pathway: An integrative cancer interactome analysis. Journal of Cellular and Molecular Medicine. 2022; 26: 2049–2062. https://doi.org/10.1111/jcmm.17228

[15] Hui J, Gao J, Wang Y, Zhang J, Han Y, Wei L, et al. Panax notoginseng saponins ameliorates experimental hepatic fibrosis and hepatic stellate cell proliferation by inhibiting the Jak2/ Stat3 pathways. Journal of Traditional Chinese Medicine = Chung i Tsa Chih Ying Wen Pan. 2016; 36: 217–224. https://doi.org/10.1016/s0254-6272(16)30030-9

[16] Benbow JH, Marrero E, McGee RM, Brandon-Warner E, Attal N, Feilen NA, et al. Hepatic stellate cell-derived exosomes modulate macrophage inflammatory response. Experimental Cell Research. 2021; 405: 112663. https://doi.org/10.1016/j.yexcr.2021.112663

[17] Parola M, Pinzani M. Liver fibrosis: Pathophysiology, pathogenetic targets and clinical issues. Molecular Aspects of Medicine. 2019; 65: 37–55. https://doi.org/10.1016/j.mam.2018.09.002

[18] Yu K, Li Q, Shi G, Li N. Involvement of epithelial-mesenchymal transition in liver fibrosis. Saudi Journal of Gastroenterology: Official Journal of the Saudi Gastroenterology Association. 2018; 24: 5–11. https://doi.org/10.4103/sjg.SJG_297_17

[19] Caligiuri A, Gentilini A, Pastore M, Gitto S, Marra F. Cellular and Molecular Mechanisms Underlying Liver Fibrosis Regression. Cells. 2021; 10: 2759. https://doi.org/10.3390/cells10102759

[20] Horn P, Tacke F. Metabolic reprogramming in liver fibrosis. Cell Metabolism. 2024; 36: 1439–1455. https://doi.org/10.1016/j.cmet.2024.05.003

[21] Wu X, Shu L, Zhang Z, Li J, Zong J, Cheong LY, et al. Adipocyte Fatty Acid Binding Protein Promotes the Onset and Progression of Liver Fibrosis via Mediating the Crosstalk between Liver Sinusoidal Endothelial Cells and Hepatic Stellate Cells. Advanced Science (Weinheim, Baden-Wurttemberg, Germany). 2021; 8: e2003721. https://doi.org/10.1002/advs.202003721

[22] Hu Y, Bao X, Zhang Z, Chen L, Liang Y, Qu Y, et al. Hepatic progenitor cell-originated ductular reaction facilitates liver fibrosis through activation of hedgehog signaling. Theranostics. 2024; 14: 2379–2395. https://doi.org/10.7150/thno.91572

[23] Zhang CY, Yuan WG, He P, Lei JH, Wang CX. Liver fibrosis and hepatic stellate cells: Etiology, pathological hallmarks and therapeutic targets. World Journal of Gastroenterology. 2016; 22: 10512–10522. https://doi.org/10.3748/wjg.v22.i48.10512

[24] Baglieri J, Brenner DA, Kisseleva T. The Role of Fibrosis and Liver-Associated Fibroblasts in the Pathogenesis of Hepatocellular Carcinoma. International Journal of Molecular Sciences. 2019; 20: 1723. https://doi.org/10.3390/ijms20071723

[25] Sufleţel RT, Melincovici CS, Gheban BA, Toader Z, Mihu CM. Hepatic stellate cells - from past till present: morphology, human markers, human cell lines, behavior in normal and liver pathology. Romanian Journal of Morphology and Embryology = Revue Roumaine De Morphologie et Embryologie. 2020; 61: 615–642. https://doi.org/10.47162/RJME.61.3.01

[26] Ying HZ, Chen Q, Zhang WY, Zhang HH, Ma Y, Zhang SZ, et al. PDGF signaling pathway in hepatic fibrosis pathogenesis and therapeutics (Review). Molecular Medicine Reports. 2017; 16: 7879–7889. https://doi.org/10.3892/mmr.2017.7641

[27] Tsuchida T, Friedman SL. Mechanisms of hepatic stellate cell activation. Nature Reviews. Gastroenterology & Hepatology. 2017; 14: 397–411. https://doi.org/10.1038/nrgastro.2017.38

[28] Zheng HC, Li J, Shen DF, Yang XF, Zhao S, Wu YZ, et al. BTG1 expression correlates with pathogenesis, aggressive behaviors and prognosis of gastric cancer: a potential target for gene therapy. Oncotarget. 2015; 6: 19685–19705. https://doi.org/10.18632/oncotarget.4081

[29] Liu C, Tao T, Xu B, Lu K, Zhang L, Jiang L, et al. BTG1 potentiates apoptosis and suppresses proliferation in renal cell carcinoma by interacting with PRMT1. Oncology Letters. 2015; 10: 619–624. https://doi.org/10.3892/ol.2015.3293

[30] Zhu R, Li W, Xu Y, Wan J, Zhang Z. Upregulation of BTG1 enhances the radiation sensitivity of human breast cancer in vitro and in vivo. Oncology Reports. 2015; 34: 3017–3024. https://doi.org/10.3892/or.2015.4311

[31] Wan L, Chen X, Deng J, Zhang S, Tu F, Pei H, et al. Plasma exosome-derived B-cell translation gene 1: a predictive marker for the prognosis in patients with non-small cell lung cancer. Journal of Cancer. 2021; 12: 1538–1547. https://doi.org/10.7150/jca.52320

[32] Zhao X, Chen GQ, Cao GM. Abnormal expression and mechanism of miR-330-3p/BTG1 axis in hepatocellular carcinoma. European Review for Medical and Pharmacological Sciences. 2019; 23: 6888–6898. https://doi.org/10.26355/eurrev_201908_18728

[33] Lu K, Liu C, Tao T, Zhang X, Zhang L, Sun C, et al. MicroRNA-19a regulates proliferation and apoptosis of castration-resistant prostate cancer cells by targeting BTG1. FEBS Letters. 2015; 589: 1485–1490. https://doi.org/10.1016/j.febslet.2015.04.037

[34] Wang D, Yan C. MicroRNA-208a-3p participates in coronary heart disease by regulating the growth of hVSMCs by targeting BTG1. Experimental and Therapeutic Medicine. 2022; 23: 71. https://doi.org/10.3892/etm.2021.10994

[35] Ogawa S, Ochi T, Shimada H, Inagaki K, Fujita I, Nii A, et al. Anti-PDGF-B monoclonal antibody reduces liver fibrosis development. Hepatology Research : the Official Journal of the Japan Society of Hepatology. 2010; 40: 1128–1141. https://doi.org/10.1111/j.1872-034X.2010.00718.x

[36] Wang X, Gao Y, Li Y, Huang Y, Zhu Y, Lv W, et al. Roseotoxin B alleviates cholestatic liver fibrosis through inhibiting PDGF-B/PDGFR-β pathway in hepatic stellate cells. Cell Death & Disease. 2020; 11: 458. https://doi.org/10.1038/s41419-020-2575-0

[37] Tang YX, Liu M, Liu L, Zhen BR, Wang TT, Li N, et al. Lipophilic Constituents in *Salvia miltiorrhiza* Inhibit Activation of the Hepatic Stellate Cells by Suppressing the JAK1/STAT3 Signaling Pathway: A Network Pharmacology Study and Experimental Validation. Frontiers in Pharmacology. 2022; 13: 770344. https://doi.org/10.3389/fphar.2022.770344

[38] Cao G, Zhu R, Jiang T, Tang D, Kwan HY, Su T. Danshensu, a novel indoleamine 2,3-dioxygenase1 inhibitor, exerts anti-hepatic fibrosis effects via inhibition of JAK2-STAT3 signaling. Phytomedicine : International Journal of Phytotherapy and Phytopharmacology. 2019; 63: 153055. https://doi.org/10.1016/j.phymed.2019.153055

[39] Ogata H, Chinen T, Yoshida T, Kinjyo I, Takaesu G, Shiraishi H, et al. Loss of SOCS3 in the liver promotes fibrosis by enhancing STAT3-mediated TGF-beta1 production. Oncogene. 2006; 25: 2520–2530. https://doi.org/10.1038/sj.onc.1209281